BIOCHIP JOURNAL, Vol. 2, No. 1, 73-77, March 2008

An Integrated Nanoporous Chip for Detecting Single DNA Molecules

Rafael Mulero[1] **& Min Jun Kim**[1]

[1]Department of Mechanical Engineering & Mechanics, Drexel University, Philadelphia, PA 19104, U.S.A
Correspondence and requests for materials should be addressed to M.J. Kim (mkim@coe.drexel.edu)

Accepted 16 January 2008

Abstract

We have developed a novel approach for ultra-fast DNA analysis by measurement of a parallel optical readout of DNA translocation through solid-state nanopore arrays. Parallelism is achieved through the fabrication of solid-state arrays of single-nanometer resolution pores and the simultaneous optical readout of DNA translocation utilizing scanning confocal microscopy. The optical readout of the arrays circumvents the previously necessary direct electrical addressing of each pore, reducing the method's complexity. We present new nanofabrication techniques to create optipore arrays in 50 nm thick silicon nitride membranes using *scanning* transmission electron microscopy (STEM) and discuss our progress toward an ultra-fast high throughput DNA analysis.

Keywords: DNA, Ionic current blockade, Optical readout, Optipore array, STEM

Introduction

The α-hemolysin protein nanopore is an archetype for the rapid characterization and sequencing of nucleic acid molecules using high-resolution analysis based on an electrical read-out[1-4]. However, due to the difficulties in forming α-hemolysin nanopores in lipid bilayers and tuning the dimensions of the heptameric pores, there are many technical constraints in investigating the structures, dynamics, and interactions of DNA/RNA molecules electrophoretically translocating through α-hemolysin nanopores. One of which is the pores' limiting constriction composed of alternating lysine and glutamate residues forming a bottleneck approximately 13 angstroms across[1,2]. As a result of this limitation, the pores are large enough to allow the passage of single-stranded DNA, but too small to accommodate double-stranded DNA.

An alternative method over the use of protein channels is the use of solid-state pores. These offer several advantages over phospholipid-embedded protein channels. The solid-state pores can be tuned in size with nanometer precision and also display improved mechanical, chemical and electrical stability. This lack of stability of protein channels is evident in α-hymolysin, where they readily diffuse in the bilayer leading to a destabilization of the membrane. Furthermore, and of utmost importance, solid-state pores realize the possibility of complimenting electrical measurements using optical-based readout methods.

Recently, new fabrication approaches to solid-state nanopores in free-standing Si_3N_4 and SiO_2 films have been developed utilizing ion beam sculpting[5], transmission electron microscopy (TEM)[6-8], and focused ion beam (FIB) systems[9,10]. These techniques take advantage of feedback into the fabrication process, which enables control of the synthesized pores' dimensions at the single nanometer length scale.

Single solid-state nanopores provide a fast, reliable, and accurate DNA analysis for a variety of sample types[11]. Single pores are, however, delimited in throughput by the sampling speed of their data signal readout systems so that a large number of DNA translocating events cannot be achieved rapidly. An evident solution for ultra-fast high throughput DNA sequencing is to use nanopore arrays, which take advantage of the parallel optical readout of DNA electrophoretically driven through hundreds of nanoscale-sized pores. This parallelism is achieved by the fabrication of high-density, solid-state nanopore arrays.

Results and Discussion

Fabrication and Characterization

Using the TEM nanopore fabrication technique developed by Dekker, Timp, and coworkers[6-8,12,13], we have fabricated solid-state optipore arrays in thin Si_3N_4 membranes. Through optimization of the electron irradiation parameters, nearly circular nanopores with diameters in the range of 2-25 nm were fabricated. We further characterized the ionic conductance of

the different diameter pores, and found a linear relationship of the conductivity using the cross-sectional area of a pore as observed using TEM. We report on the translocation of λ-DNA molecules through a 6 nm pore, as detected using a two-electrode patch clamp technique[4,14-16] and additionally show the ability of an optical readout by translocating 150 bp fluorescently labeled DNA through a 3×3 optipore array.

An optimal low-density optipore array (2×2, and 3×3) has been integrated into a monolithic silicon-based chip using an automated scanning transmission electron microscope (STEM) in which the array is precisely determined by the patterning of the beam scanning. An automated patterning of optipores is possible by running the microscope in STEM mode and directly addressing the scan coils to deflect the beam by a desired amount[7]. Such a method is possible by direct beam control through either an analytical x-ray acquisition system or from a dedicated e-beam lithography system such as an NPGS modified for use on a STEM system. In such a system, the probe shift is calibrated for *x*-*y* translation and the electron beam dwell times can be specified for various points on the sample. Using this method, it is possible to produce as many accurately positioned pores as is needed on the substrate. Figure 1 shows an array where each nanopore has a diameter of 8 nm. TEM tomography[8] reveals that all of these pores have an identical three-dimensional structure. This verifies that the identical structure of all the pores demonstrates the robust nature of STEM fabrication. A rendering of a 2×2 nanopore array fabricated on a free-standing silicon nitride window framed by a $5 \times 5\,\text{mm}^2$ silicon chip is shown in Figure 1c.

We have characterized the ionic conductivity of our optipores by performing a set of current-voltage (I-V) measurements at different ionic strengths. In all cases, the optipores exhibit ohmic behavior in the range of ± 0.5 V. Figure 2 shows a linear dependence of the pore diameter on the square root of the ionic conductivity, indicating the effect of reducing the size of the pore on the resistance to ion transfer. The ratio of the slopes for the two lines obtained for different concentrations is 2.21, compared to 2.23 expected for a five-fold increase in electrolyte concentration. Conductivity measurements of a typical 3×3 optipore array with $d = 9.3 \pm 0.8$ nm yield 3.6×10^{-7} S, which is in agreement with the expected conductivity of nine pores of the same diameter (3.3×10^{-7} S), as shown in Figure 2.

Observation of DNA Translocation Events in a Single Nanopore

By monitoring the conductance of a voltage-biased

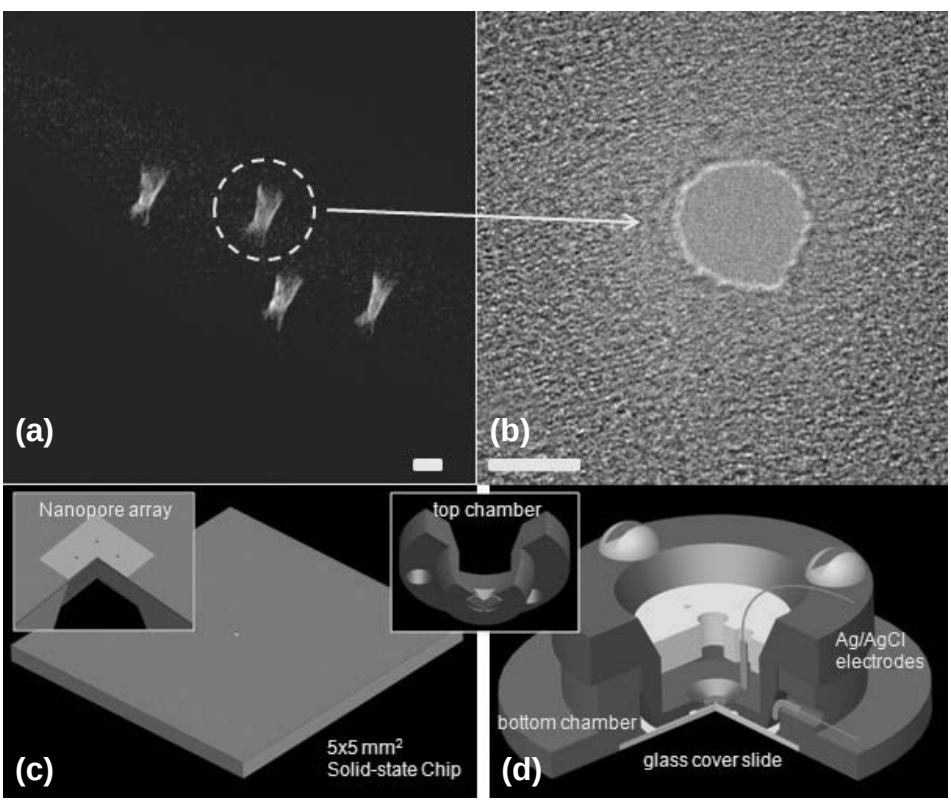

Figure 1. (a) A tilted TEM tomographic view of a solid-state 2×2 optipore array. (b) A typical solid-state nanopore on the optipore array. The scale bars are 5 nm. (c) Rendering of a $5 \times 5\,\text{mm}^2$ silicon nitride on a silicon chip. (Inset c) Close-up 3/4 sectional view of a free-standing silicon nitride window with a 2×2 nanopore array. (d) Rendering with quarter section removed from the five-piece flow-cell assembly used during both optical and electrical readout analyses. (Inset d) Nanopore array chip adhered to the upper chamber of the flow cell.

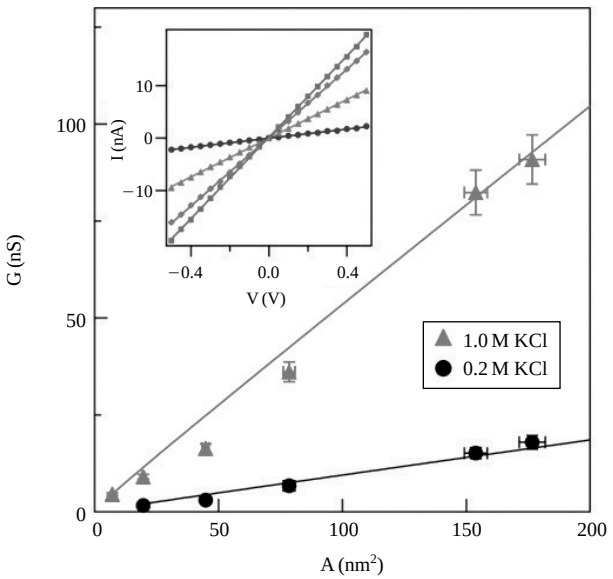

Figure 2. Ionic conductance (G) of solid-state nanopores of various cross-sectional areas in 1.0 M (triangles) and 0.2 M (circle) KCl solution (+10 mM TRIS buffer, pH 8.5). The lines represent fits assuming a cylindrical pore geometry, revealing a pore length of $l = 30 \pm 2$ nm. Inset: I-V curves obtained from 1.0 M KCl for nanopores with average diameters (±5%) of 12 nm (squares), 10 nm (diamonds), 7 nm (triangles), and 3 nm (circles).

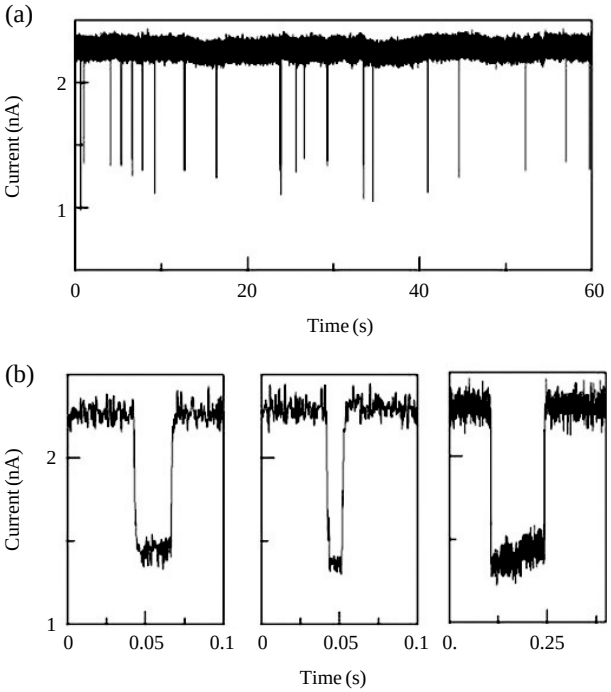

Figure 3. (a) Measured ionic current (in 1.0 M KCl) of a 6 nm diameter solid-state nanopore at a driving voltage of 500 mV, slowing the frequent drops in the current corresponding to translocation of λ-DNA ([λ-DNA]~1 mg/mL). (b) Three individual events are shown at increasing time resolutions. The abrupt changes in the current upon DNA entry and exit from the nanopore occur in less than 50 μs.

pore, we detect the translocation of λ-DNA at 500 mV of applied potential across a 6 nm solid-state pore. The event time for each translocation varies widely, as do the current fluctuations.

Signals were low-pass filtered at 20 KHz using a Butterworth filter and digitized at 100 KHz (12 bit). Figure 3 displays ion current blockades produced by applying λ-DNA ([λ-DNA]~1 mg/mL) to the negative chamber of a chip (the "cis" chamber) containing a single 6 nm nanopore. Upon the addition of the DNA, the ion current developed sharp blockade spikes, similar to the ones observed in α-hemolysin experiments[4]. A typical set of ion current blockades is shown in Figure 3.

High Throughput Detection of Single Molecules through an Optipore Array

The direct electrical addressing of each pore in the optipore arrays is perturbed by ion current blockages in neighboring pores. To demonstrate the functionality of the arrays, we performed DNA translocation experiments using a scanning confocal microscope. As TMR (tetramethyl-rhodamine)-labeled 150 bp single-stranded DNA (PAGE purified) from a 0.01 μM solution were translocated through the nanopore array, their fluorescence readout was measured using an iXon CCD camera. Thus, combining DNA translocation through an optipore array with its optical readout capability presents us with novel geometries for the massive parallelism of ultra-fast DNA analysis through nanopores.

An optimal array made of 6 nm diameter nanopores, shown in Figure 4, is fabricated in a silicon nitride membrane, which has a refractive index of approximately 2.03. Unlike metal-deposited membranes, fluorescently labeled DNA in the "cis" chamber are completely illuminated by the excitation light, so that the entire DNA sample is fluorescing at the same time. We add a pinhole in the light path to reject the background haze caused by out-of-focus fluorescent light. The resulting images captured by the scanning confocal microscope show six translocating events of single-stranded DNA through the 3×3 optipore array shown in Figure 4. Further investigation of the optical signal readout method is needed, and future studies will use a TIRF system instead of a confocal microscope because of the low background conditions, and hence, higher signal/noise ratio.

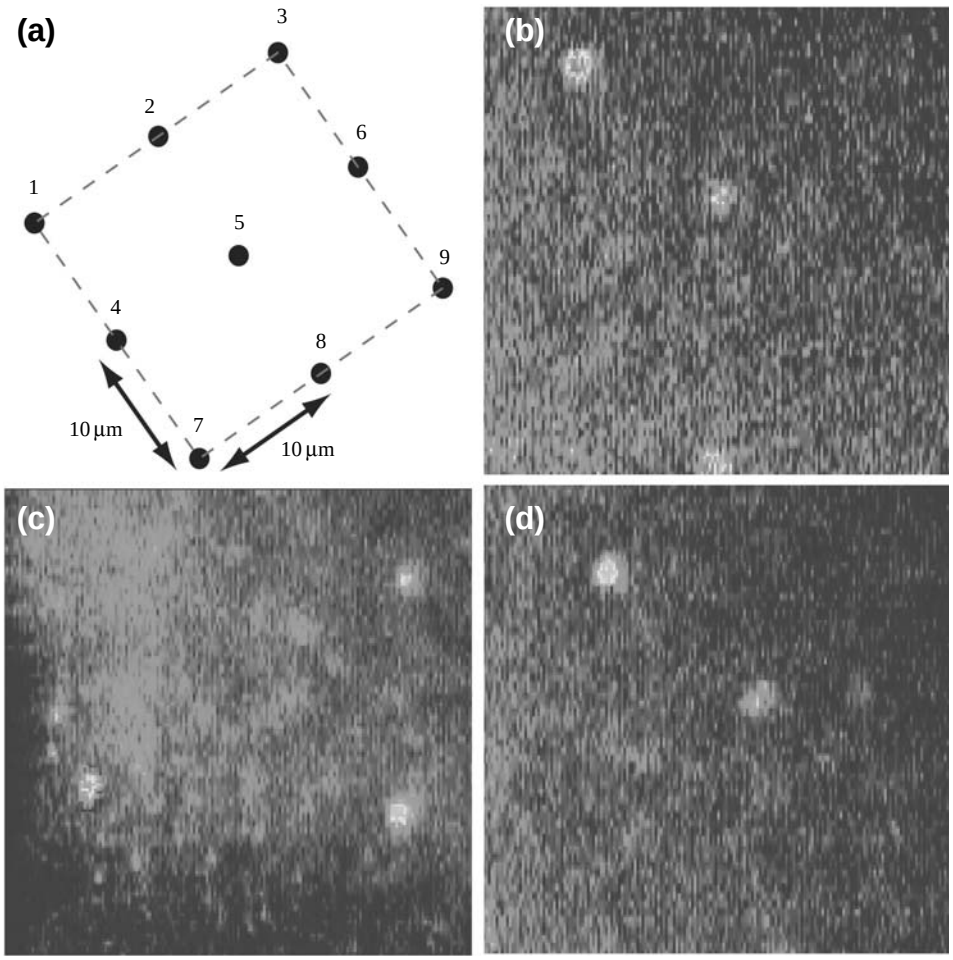

Figure 4. Confocal microscopic images translocating ssDNA through a 3 × 3 optipore array. (a) Schematic of the 3 × 3 optipore array (10 μm distances between 5 nm diameter pores). (b) Fluorescence signals from the 4th, 6th, and 8th pores. (c) Fluorescence signals from the 2nd, 5th, and 7th pores. (d) Fluorescence signals from the 2nd and 5th pores.

Conclusions

In summary, we have developed and optimized a procedure for rapid nanopore fabrication in Si_3N_4 membranes. Our procedure yields highly tunable nanopores in the range of 2-20 nm, which can be used for nucleic acids and protein analysis. We achieve uniformity of typically 0.5 nm (STD) in the optipore arrays. An important attribute of our procedure is that the fabrication time is typically less than 60 seconds, which favorably compares with previous reports[5,6]. This makes it ideal for the fabrication of high-density optipore arrays with a uniform size distribution, and therefore opening up to a wide range of possibilities for a highly parallelized DNA and protein analysis using a combination of electrical and optical detection.

Materials and Methods

Each nanopore chip was mounted in a custom-built flow cell to enable low-noise electrical and optical measurements. Once the nanopore array chip is completely fabricated, it is adhered to the five-piece flow cell (Figure 1d) consisting of two chambers bridged by the nanopore array chip, an electrode holder, and a glass slide. The chamber consists of upper "cis" and lower "trans" portions fabricated from polytetrafluoroethylene (PTFE), forming miniature electrolytic fluid chambers accessible by fluid lines. During experimentation, both chambers are filled with a conducting KCl solution. The electrode holder used to hold the Ag/AgCl anode tops the upper chamber and defines the anode's contact exposure to the ionic fluid. The circular glass cover slip allows a direct optical path to the chip during optical-based readouts and is sealed to the bottom of the lower chamber using a silicone elastomer epoxy. The same epoxy is also used to seal the nanopore array chip to the bottom of the upper chamber (Figure 1d inset). The electrodes are connected to a Molecular Devices Axopatch 200B patch clamp amplifier, which clamps a potential across the nanopore array while recording

the resulting ionic current flow. The electrical data is sampled at 100-250 kHz, digitized using a MD Digidata 1440A digitizer, and analyzed using pClamp 10.1 software. To minimize any ambient EMF-induced noise in the data signal, the entire flow cell and patch clamp headstage are located inside a copper Faraday cage.

Acknowledgements

We acknowledge stimulating conversation and support from Drs. Joshua Edel, John Kasianowicz, and Joey Robertson. Special thanks should be given to the staff at the Nanofabrication Center at the University of Minnesota for technical assistance. We acknowledge financial support from National Science Foundation DGE #0654313.

References

1. Song, L. *et al.* Structure of staphylococcal alpha-hemolysin, a heptameric transmembrane pore. *Science* **274**, 1859-1866 (1996).
2. Kasianowicz, J.J., Brandin, E., Branton, D. & Deamer, D.W. Characterization of individual polynucleotide molecules using a membrane channel. *Proc. Natl. Acad. Sci. USA* **93**, 13770-13773 (1996).
3. Akeson, M., Branton, D., Kasianowicz, J.J., Brandin, E. & Deamer, D.W. Microsecond time-scale discrimination among polycytidylic acid, polyadenylic acid, and polyuridylic acid as homopolymers or as segments within single RNA molecules. *Biophys. J.* **77**, 3227-3233 (1999).
4. Meller, A., Nivon, L. & Branton, D. Voltage-driven DNA translocations through a nanopore. *Phys. Rev. Lett.* **86**, 3435-3438 (2001).
5. Li, J. *et al.* Ion-beam sculpting at nanometer length scale. *Nature* **412**, 166-169 (2001).
6. Storm, A.J., Chen, J.H., Ling, X.S., Zandbergen, H.W. & Dekker, C. Fabrication of solid-state nanopores with single-nanometer precision. *Nature Materials* **2**, 537-540 (2003).
7. Kim, M.J., Wanunu, M., Bell, D.C. & Meller, A. Rapid fabrication of uniformly sized nanopores and nanopore arrays for parallel DNA analysis. *Advanced Materials* **18**, 3149-3153 (2006).
8. Kim, M.J., McNally, B., Murata, K. & Meller, A. Characteristics of solid-state nanopores fabricated using a transmission electron microscope. *Nanotechnology* **18**, 205302-205306 (2007).
9. Lo, C.J., Aref, T. & Bezryadin, A. Fabrication of symmetric sub-5 nm. nanopores using focused ion and electron beams. *Nanotechnology* **17**, 3264-3267 (2006).
10. Chasin, G.A.T. *et al.* Single molecule spectroscopy using nanoporous membranes. *Nano Letters* **7**, 2901-2906 (2007).
11. Smeets, R.M.M. *et al.* Salt dependence of ion transport and DNA translocation through solid-state nanopores. *Nano Letters* **6**, 89-95 (2006).
12. Wu, M.-Y., Krapf, D., Zandbergen, M., Zandbergen, H. & Batson, P.E. Formation of nanopores in a SiN/SiO_2 membranes with an electron beam. *Appl. Phys. Lett.* **87**, 113106-113108 (2005).
13. Heng, J.B. *et al.* Sizing DNA using a nanometer-diameter pore. *Biophys J.* **90**, 1098-1106 (2004).
14. Bates, M., Burns, M. & Meller, A. Dynamics of DNA molecules in a membrane channel probed by active control techniques. *Biophys. J.* **84**, 2366-2372 (2001).
15. Mathé, J., Visram, H., Viasnoff, V., Rabin, Y. & Meller, A. Nanopore unzipping of individual DNA hairpin molecules. *Biophys. J.* **87**, 3205-3212 (2004).
16. Mathé, J., Aksimentiev, A., Nelson, D.R., Schulten, K. & Meller, A. Orientation discrimination of single-stranded DNA inside the alpha-hemolysin membrane channel. *Proc. Natl. Acad. Sci. USA* **102**, 12377-12382 (2005).